Pelvic Inflammatory Disease: Multimodality Imaging Approach with Clinical-Pathologic Correlation[1]

Margarita V. Revzin, MD, MS
Mahan Mathur, MD
Haatal B. Dave, MD
Matthew L. Macer, MD
Michael Spektor, MD

Abbreviation: PID = pelvic inflammatory disease

RadioGraphics 2016; 36:1579–1596

Published online 10.1148/rg.2016150202

Content Codes: CT GU MR OB US

[1]From the Department of Diagnostic Radiology (M.V.R., M.M., H.B.D., M.S.) and Department of Obstetrics and Gynecology and Reproductive Sciences (M.L.M.), Yale University School of Medicine, 333 Cedar St, PO Box 208042, Room TE-2, New Haven, CT 06520. Presented as an education exhibit at the 2014 RSNA Annual Meeting. Received June 27, 2015; revision requested December 21; revision received January 21, 2016; accepted January 28. For this journal-based SA-CME activity, the authors, editor, and reviewers have disclosed no relevant relationships. Address correspondence to M.S. (e-mail: *michael.spektor@yale.edu*).

See discussion on this article by Patlas (pp 1597–1599).

SA-CME LEARNING OBJECTIVES

After completing this journal-based SA-CME activity, participants will be able to:

- Describe the anatomy of the female genital tract and the CT features of early- and late-stage PID.
- Identify the CT imaging findings associated with complications of PID.
- Describe the CT mimics of PID, including their imaging characteristics and differentiating features.

See www.rsna.org/education/search/RG.

Pelvic inflammatory disease (PID) is a common medical problem, with almost 1 million cases diagnosed annually. Historically, PID has been a clinical diagnosis supplemented with the findings from ultrasonography (US) or magnetic resonance (MR) imaging. However, the diagnosis of PID can be challenging because the clinical manifestations may mimic those of other pelvic and abdominal processes. Given the nonspecific clinical manifestations, computed tomography (CT) is commonly the first imaging examination performed. General CT findings of early- and late-stage PID include thickening of the uterosacral ligaments, pelvic fat stranding with obscuration of fascial planes, reactive lymphadenopathy, and pelvic free fluid. Recognition of these findings, as well as those seen with cervicitis, endometritis, acute salpingitis, oophoritis, pyosalpinx, hydrosalpinx, tubo-ovarian abscess, and pyometra, is crucial in allowing prompt and accurate diagnosis. Late complications of PID include tubal damage resulting in infertility and ectopic pregnancy, peritonitis caused by uterine and/or tubo-ovarian abscess rupture, development of peritoneal adhesions resulting in bowel obstruction and/or hydroureteronephrosis, right upper abdominal inflammation (Fitz-Hugh–Curtis syndrome), and septic thrombophlebitis. Recognition of these late manifestations at CT can also aid in proper patient management. At CT, careful assessment of common PID mimics, such as endometriosis, adnexal torsion, ruptured hemorrhagic ovarian cyst, adnexal neoplasms, appendicitis, and diverticulitis, is important to avoid misinterpretation, delay in management, and unnecessary surgery. Correlation with the findings from complementary imaging examinations, such as US and MR imaging, is useful for establishing a definitive diagnosis.

Introduction

Pelvic infection is the most frequent gynecologic cause of emergency department visits, with the number of such visits approaching 350 000 per year in the United States (1). As many as 70% of the adolescent patients with pelvic inflammatory disease (PID) are diagnosed in the emergency department (2), and nearly 1 million patients with PID are diagnosed annually in the United States (3). Despite its relative frequency, pelvic infection can represent a diagnostic dilemma because the symptoms are often mild and nonspecific and may not direct the clinician toward the correct diagnosis. In this setting, computed tomography (CT) of the abdomen and pelvis is frequently performed as the initial diagnostic imaging examination, which allows the referring physicians to promptly assess for a broad spectrum of pathologic conditions, such as appendicitis, diverticulitis, adnexal torsion, and bowel obstruction. A thorough understanding of the CT findings of early and late manifestations of PID is therefore crucial

TEACHING POINTS

- Posterior extension of inflammatory adnexal or tubal disease often causes thickening of the uterosacral ligaments and increased haziness of the presacral and perirectal fat planes.
- Salpingitis should be suspected at CT when the fallopian tubes are thickened, measuring more than 5 mm in axial dimension, and show enhancing walls. Associated free fluid may be depicted within the cul-de-sac. For the diagnosis of PID, the CT finding of tubal thickening was found to have a high specificity of 95%.
- A pathognomonic finding of hydrosalpinx at US, CT, and MR imaging is a "cogwheel" appearance of the tube when imaged in cross section, an appearance that is due to thickened longitudinal folds. Otherwise, the wall of the tube is thin and shows no appreciable enhancement or hyperemia.
- Anterior displacement of the broad ligament, because of the posterior position of the mesovarium, may allow differentiation of a tubo-ovarian abscess from a pelvic abscess of other origin. In addition, pelvic abscesses originating from the appendix, colon, and bladder tend to have thicker walls and may be located further from the adnexa.
- Common CT imaging features that distinguish ovarian torsion from PID include an enlarged ovary with a diameter of more than 5 cm, a lack of ovarian contrast enhancement, and uterine deviation toward the affected side.

to properly interpret the findings from these examinations and aid in the establishment of a definitive diagnosis.

In this article, the anatomy of the uterus, ovaries, and fallopian tubes is reviewed, as well as their supporting structures and related spaces; and their involvement in pelvic inflammatory processes is described. Expected CT findings in the early and late stages of PID are described, with a specific focus on cervicitis, endometritis, salpingitis, oophoritis, pyosalpinx, hydrosalpinx, tubo-ovarian abscess, and pyometra. Complications and late sequelae of PID are reviewed, including tubal damage, uterine and tubo-ovarian abscess rupture, development of abdominal and pelvic peritoneal adhesions, right upper abdominal inflammation (Fitz-Hugh–Curtis syndrome), and ovarian vein thrombophlebitis. Finally, the CT mimics of PID, such as endometriosis, adnexal torsion, ruptured hemorrhagic ovarian cyst, adnexal neoplasms, appendicitis, and diverticulitis, are reviewed. The findings from other complementary imaging modalities, such as ultrasonography (US) and magnetic resonance (MR) imaging, are correlated with the CT findings, and images of intraoperative procedures and histopathologic specimens are provided.

Background

PID encompasses all upper genital tract infections, including cervicitis, endometritis, salpingitis, oophoritis, hydrosalpinx, tubo-ovarian abscess, and peritonitis (4). The cause of PID is typically an ascending lower genital tract infection. The proposed pathway of spread of causative agents is usually by direct upward extension of infection from the vagina to the cervix, followed by the fallopian tubes and ovaries, and, finally, to the peritoneal cavity. Hematogenous spread and extension of infection from adjacent organs are less common causes of PID. The etiology of PID has been linked to sexually transmitted microorganisms such as *Chlamydia trachomatis, Neisseria gonorrhoeae, Mycoplasma genitalium,* and gram-negative bacteria (4). Polymicrobial infections account for 30%–40% of reported cases of PID (5,6). Tuberculosis and actinomycosis occur much less frequently.

Common clinical symptoms of PID include pelvic pain, fever, vaginal discharge, dyspareunia, leukocytosis, and other vague constitutional symptoms. Major risk factors include a history of multiple sexual partners, young age, a prior uterine procedure, and intrauterine devices (5).

The clinical history and the findings at physical examination, in conjunction with US findings, are usually diagnostic. However, given the vague and nonspecific presenting symptoms, CT is often the first imaging examination performed. CT is useful in assessing the extent of peritoneal disease, evaluating chronic or recurrent PID, evaluating for disease complications, and excluding other differential diagnostic considerations. MR imaging is useful in the delineation of the uterine and adnexal structures and the differentiation of PID from other pathologic processes. Laparoscopy is not optimal as a diagnostic tool because of its invasive nature.

In the absence of complications, PID is generally treated conservatively with a short course of oral antibiotic therapy. Patients with complicated PID frequently require hospitalization, with intravenous administration of antibiotic therapy, in addition to percutaneous or surgical drainage of pelvic abscesses if present.

Anatomy

The uterus is located in the pelvis between the urinary bladder and the rectum. The body of the uterus lies between the layers of the broad ligament and is freely movable. The peritoneal reflections covering the uterus and bladder form the vesicouterine pouch, and those covering the uterus and rectum form the rectouterine pouch. The broad ligament assists in fixing the uterus in place and represents a double layer of peritoneum (mesentery) that extends from the sides of the uterus to the lateral walls and floor of the pelvis. The portion of the broad ligament that forms the mesentery of the

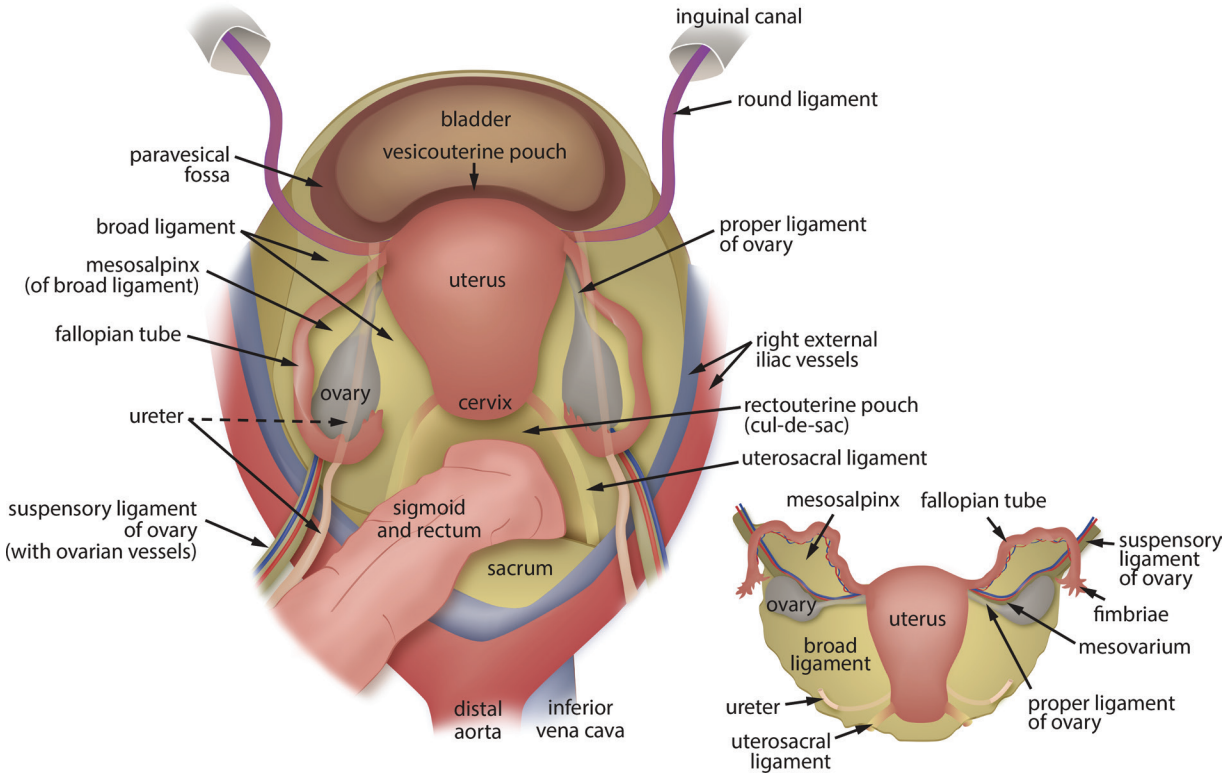

Figure 1. Diagrams showing relative female pelvic anatomy.

uterine tube (fallopian tube) is termed the *mesosalpinx*. The ovaries lie close to the fimbriae, the distal ends of the fallopian tubes. The superolateral margin of the broad ligament forms the suspensory ligament of the ovary, which extends over the ovarian vessels. The ligament of the ovary (proper ligament of the ovary) attaches to the uterus posteroinferior to the uterotubal junction. The round ligament of the uterus attaches anteroinferior to the uterotubal junction and extends into the bilateral inguinal canals. The uterosacral ligaments course posterosuperiorly from the lateral margins of the cervix to the midportion of the sacrum. These ligaments provide both passive and active support, allowing the uterus to maintain its central position in the pelvic cavity (Fig 1) (7). All of the aforementioned structures may be involved in pelvic infectious or inflammatory processes, which usually result in thickening and hyperemia of the structures.

CT Technique

A CT examination is frequently performed in patients with nonspecific symptoms, as well as in patients with suspected pelvic pathologic conditions and equivocal US findings. In our institution, emergent standard CT of the abdomen and pelvis is usually performed on a 64-section CT scanner (GE Healthcare, Milwaukee, Wis), with the scan obtained from the level of the dome of the diaphragm to the level of the pubic symphysis.

Administration of diluted oral barium contrast material is helpful in the distinction of the gastrointestinal tract from adnexal structures. However, a new trend is to eliminate the routine use of oral contrast material for CT in the emergency department, because investigators have shown that its elimination does not compromise diagnosis in the acutely ill patient and successfully decreases the length of stay in the emergency department (8). Intravenous contrast material administration is preferred because it allows better delineation of the uterus and adnexal structures, as well as assessment of endometrial, cervical, and tubal perfusion. At our institution, the examinations were performed with CT scanners (LightSpeed VCT or Discovery CT750 HD; GE Healthcare). All examinations are performed in the portal venous phase. The portal venous phase images were acquired by using a scanning delay of 70 seconds after the injection of 85 mL of iohexol (Omnipaque 300; GE Healthcare) at a rate of 2–3 mL/sec. The CT parameters were as follows: section thickness, 5 mm; reconstruction interval, 0.625 mm; pitch, 0.6; voltage, 120 kVp with automatic exposure control (Auto or Smart mA; GE Healthcare); and noise index, 22. The data were reconstructed by using a standard algorithm. Coronal and sagittal multiplanar

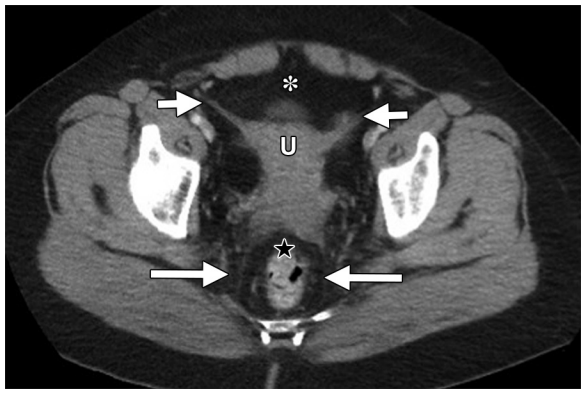

Figure 2. Normal pelvic anatomy. Axial contrast-enhanced CT image shows a normal appearance of the uterosacral ligaments (long arrows), round ligaments (short arrows), clear fat in the rectouterine pouch (★), and anterior pelvic fat (*), as well as normal size of the uterus *(U)*.

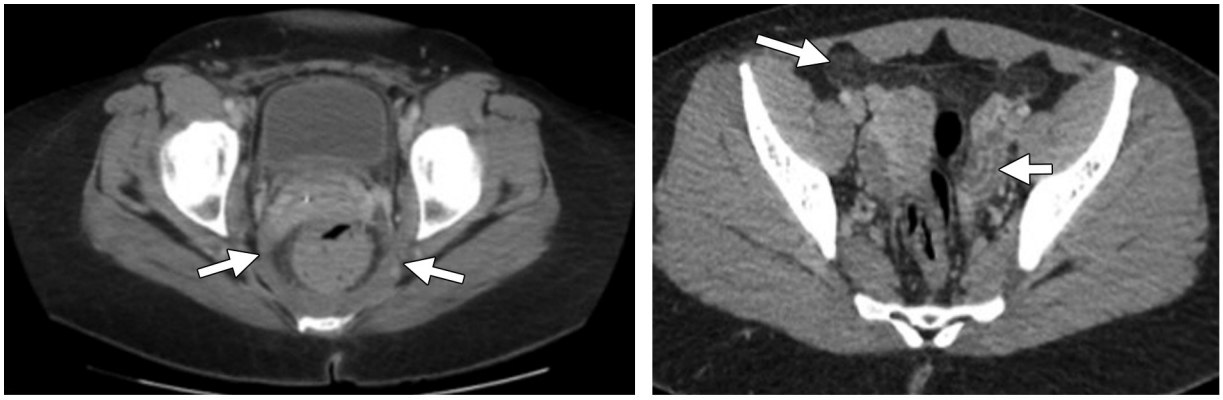

a. **b.**

Figure 3. Early PID: general CT findings in two different patients. **(a)** Axial contrast-enhanced CT image of a 32-year-old woman presenting with pelvic pain and low-grade fever shows thickened and edematous uterosacral ligaments (arrows). **(b)** Axial contrast-enhanced CT image of a 25-year-old woman with cervical motion tenderness shows marked anterior pelvic fat stranding (long arrow) and thickening of the left fallopian tube (short arrow). PID was confirmed clinically on the basis of the patient's microbiologic results.

reconstructions, which are useful for evaluating complex female pelvic anatomy, are created by using source data obtained in the axial plane. Oral contrast material was prepared with 25 mL of iohexol (Omnipaque 350; GE Healthcare) diluted in 875 mL of water. Oral contrast material was administered starting 90 minutes before the examination. It is important to note that a patient's pregnancy status must be determined before performing CT in any premenopausal female.

Overview of General CT Findings of PID

PID represents a clinical continuum of the infectious conditions that affect the upper genital tract. Because there is a gradual progression from one condition to the next, no true separation exists between each entity, and therefore considerable overlap exists in the general imaging features of each of these infectious processes. After a review of the general imaging features encountered with PID, specific entities will be reviewed individually.

The most common general CT findings of PID described in the literature are thickening of the uterosacral ligaments, obliteration of fascial planes, free fluid in the cul-de-sac, loss of definition of the uterine border, pelvic fat infiltration or haziness and pelvic edema, reactive lymphadenopathy, and signs of peritonitis. The uterosacral ligaments are paired structures that extend from the lower uterine segment to the mid sacrum and are best seen on axial cross-sectional images. The normal thickness of the uterosacral ligaments is subjective and has not yet been established on CT images (Fig 2). Posterior extension of inflammatory adnexal or tubal disease often causes thickening of the uterosacral ligaments and increased haziness of the presacral and perirectal fat planes (Fig 3) (9). Pelvic fat haziness refers to increased attenuation of the pelvic fat when compared with retroperitoneal fat. Pelvic fat haziness is one of the most sensitive findings of acute PID and is seen in as many as 65% of patients (10,11). Pelvic peritonitis refers to increased attenuation and marked stranding of the pelvic fat with peritoneal enhancement.

PID often is accompanied by reactive lymphadenopathy affecting the paraaortic lymphatic chain at the level of the renal hila. This lymph-

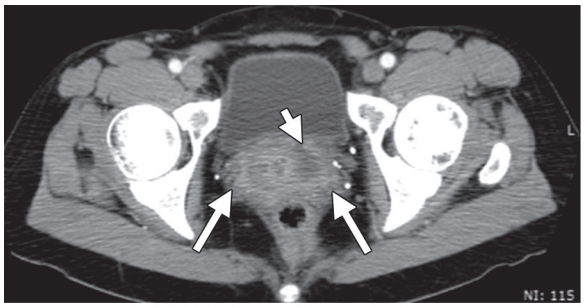

a.

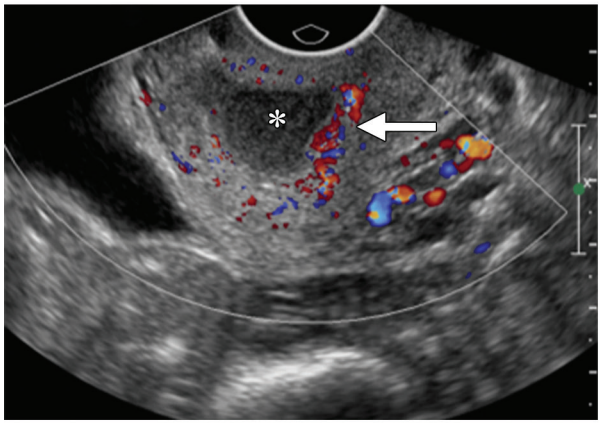

b.

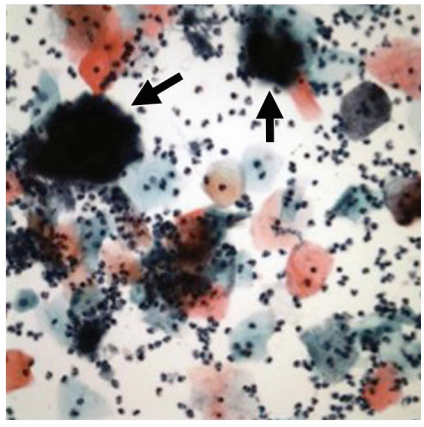

c.

Figure 4. Early PID: cervicitis in a 54-year-old woman with pelvic pain and vaginal discharge. **(a)** Axial contrast-enhanced CT image shows an enlarged edematous uterine cervix (long arrows) with loss of the surrounding fat planes and with complex fluid (short arrow) in the enhancing endocervical canal. **(b)** Transverse transvaginal color Doppler US image obtained 5 days later shows the fluid-filled distended endocervical canal (*) with surrounding hyperemia (arrow). **(c)** Photomicrograph of Papanicolaou smear shows the "fluffy cotton" appearance of *Actinomyces* (arrows), a finding compatible with acute cervicitis. (Papanicolaou stain; original magnification, ×200.)

adenopathy is caused by the course of drainage of the ovarian and salpingian lymphatic vessels along the gonadal veins (12,13).

Additional imaging findings predictive of PID are *(a)* hepatic capsular enhancement on the late arterial phase images and *(b)* fallopian tube thickening of more than 5 mm. The combination of these two findings had a sensitivity of 71.9%, specificity of 81.3%, and accuracy of 76.6% (10). The specificity of the tubal thickening sign alone has been reported to be as high as 95% (11).

Early Stage of PID

Cervicitis

Cervicitis, defined as inflammation of the uterine cervix, can be divided into two major categories: noninfectious and infectious cervicitis. Infectious cervicitis represents an early form of PID. Symptoms may be subclinical or may include pelvic pressure or pain, a yellow jellylike vaginal discharge, or spotting or bleeding with intercourse (thought to be caused by the fragility of blood vessels in the infected cervix). Both CT and US may demonstrate an enlarged uterine cervix, an abnormally enhancing or hyperemic endocervical canal, and parametrial fat stranding (Fig 4). Free fluid may also be seen in the pouch of Douglas (posterior cul-de-sac). Occasionally, patients with cervicitis may develop cystic changes within the lining of the endocervical canal. The deep stroma of the cervix is usually intact. Infectious cervicitis can be differentiated from malignancy by the absence of solid enhancing components in the abnormal cervix (14,15).

Endometritis

Endometritis is defined as inflammation of the endometrial lining of the uterus. Endometritis is most commonly seen during pregnancy or in the postpartum state. In the nonobstetric population, PID and invasive gynecologic procedures are the most common causes of acute endometritis. Along with cervicitis, endometritis often represents a subclinical form of PID, with patients being asymptomatic. Findings of endometritis at CT include an increased size of the uterus caused by inflammation, the accumulation of fluid in the endometrial canal, and abnormal endometrial enhancement relative to

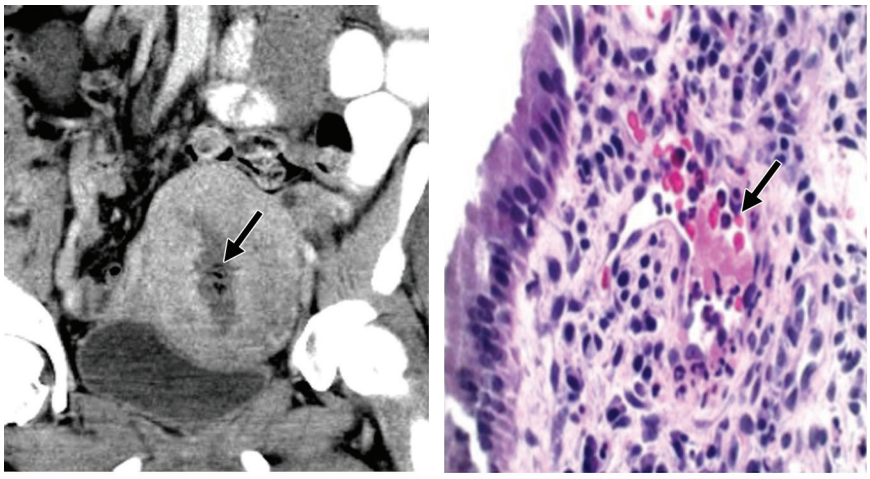

Figure 5. Early PID: endometritis in a 43-year-old woman with diabetes who presented with pelvic pain and vaginal discharge. **(a)** Coronal contrast-enhanced CT image shows an enlarged uterus, a fluid-distended endometrial canal containing foci of gas (arrow), and abnormal endometrial enhancement of more than the surrounding inner myometrium. **(b)** Low-power photomicrograph of the endometrial specimen shows numerous polymorphonuclear neutrophils (arrow) in the endometrial stroma, a finding compatible with acute endometritis. (Hematoxylin-eosin stain; original magnification, ×200.)

a. **b.**

the surrounding inner myometrium caused by mucosal hyperemia (Fig 5). A loss of the clear separation of the uterus from the adnexal and parametrial fat is also seen, which results in the development of the "indistinct uterine border" sign (16–18). This sign is nonspecific because it may also be seen with endometriosis or malignancy. The patient's age at presentation, the clinical symptoms, and the findings at endometrial biopsy may aid in the differentiation of these pathologic conditions.

Salpingitis and Tubo-ovarian Complex

Salpingitis is defined as inflammation of one or both fallopian tubes, and it is the most common early acute form of PID. The incidence of salpingitis continues to increase on a worldwide scale. The predominant population affected is young women. Among the spectrum of pathologic conditions of PID, salpingitis is associated with the highest risk of infertility and accounts for most of the ectopic pregnancies related to PID. Concomitant endometritis may occur in as many as 70%–90% of documented cases of salpingitis in nonobstetric patients (19).

In cases of salpingitis, the fallopian tubes become edematous and congested. As acute suppurative salpingitis ensues, the tubal lumen fills with pus, which subsequently spills into the peritoneal cavity and coats the serosal surface of the uterus and ovary. This event results in inflammation of the peritoneal structures. The tubal fimbriae may adhere to the ovary, resulting in salpingo-oophoritis or tubo-ovarian complex. In tubo-ovarian complex, although the ovaries and tubes partially adhere to one another, they still largely remain separate (20).

The clinical manifestations of salpingitis are diverse, ranging from no symptoms to severe pelvic pain, with poor correlation between the intensity of symptoms and the severity of tubal inflammation. Although direct laparoscopy is the reference standard for the diagnosis of salpingitis, use of this procedure is limited because of its invasive nature and expensive cost. US is considered the first-line imaging modality in the evaluation of suspected salpingitis; however, US may only demonstrate subtle abnormalities such as tubal tortuosity, wall hyperemia, and fallopian tube thickening of more than 5 mm (10,11). When they are normal in size, the fallopian tubes measure 1–4 mm in diameter and are not regularly depicted at US or CT (21). Salpingitis should be suspected at CT when the fallopian tubes are thickened, measuring more than 5 mm in axial dimension, and show enhancing walls. Associated free fluid may be depicted within the cul-de-sac (Fig 6). For the diagnosis of PID, the CT finding of tubal thickening was found to have a high specificity of 95% (11). Salpingitis should be differentiated from secondary inflammation of the fallopian tubes as a result of nongynecologic processes such as appendicitis or diverticulitis.

Oophoritis

Oophoritis is defined as inflammation of the ovaries. It is commonly seen in combination with salpingitis and pyosalpinx, because in these processes, the tubal fimbriae may adhere to the ovary, causing secondary inflammation and infection of the ovary. The distinguishing findings of oophoritis, which can be seen at US, CT, and MR imaging, include *(a)* mild enlargement of the ovaries, measuring more than 3 cm (5,11), with hyperemia of the ovarian stroma, and *(b)* a polycystic-like appearance of the ovaries, with multiple small (2–10-mm) follicles within the increased ovarian stroma (Fig 7) (22). Abnormal enhancement of the ovary can be seen at both CT and MR imaging. Free

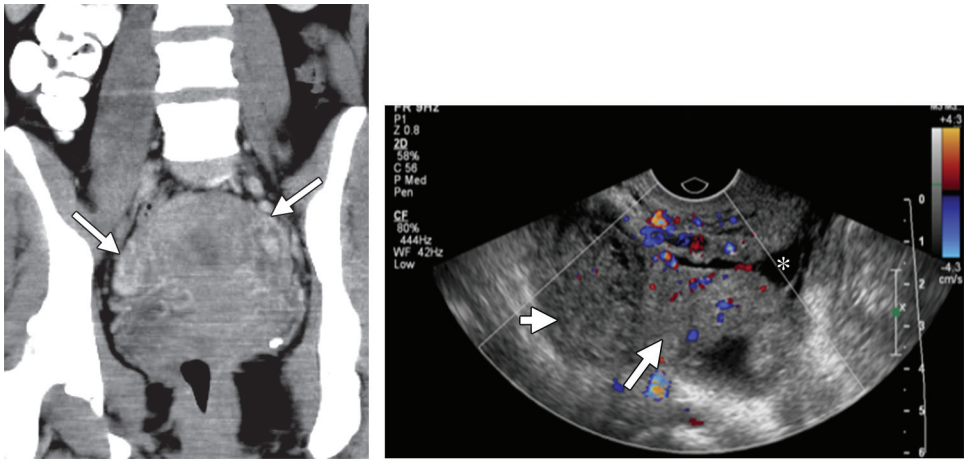

a. b.

Figure 6. Early PID: salpingitis in a 19-year-old woman presenting with lower pelvic pain, leukocytosis, and fever. **(a)** Coronal contrast-enhanced CT image shows prominent abnormally enhancing fallopian tubes (arrows) bilaterally. **(b)** Transverse transvaginal color Doppler US image of the right adnexa obtained 2 days later shows a thick-walled hyperemic fallopian tube (long arrow), as well as the adjacent right ovary (short arrow) and a small amount of free fluid (*) in the adnexa.

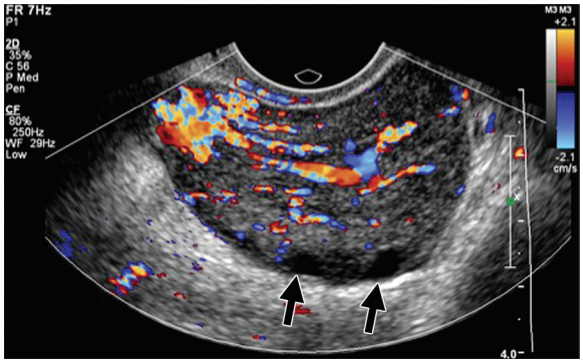

Figure 7. Early PID: oophoritis in a 24-year-old woman presenting with right lower quadrant pain. Sagittal transvaginal color Doppler US image of the right adnexa shows an enlarged, edematous, and hyperemic right ovary. Note the peripheral displacement of multiple small follicles (arrows), which gives the ovary a polycystic-like appearance.

fluid in the cul-de sac is commonly an associated finding (23). Ovarian torsion remains a major differential consideration for oophoritis, with some overlap in the imaging findings. US and MR imaging may be helpful in the evaluation of ovarian torsion; however, the findings are often nonspecific, and direct laparoscopic assessment may be warranted.

Late Stage of PID

Late or advanced PID is characterized by a moderate to severe infection of the upper genital tract and peritoneum. Advanced PID is frequently complicated by accumulation of pus and necrotic tissue in the fallopian tubes, which may extend to the ovaries and peritoneum.

Pyosalpinx

Pyosalpinx is an infection of the fallopian tubes that is complicated by tubal obstruction. The fimbrial end is usually obstructed by adhesions within and around the tube as a result of tubal inflammation. This obstruction results in accumulation of trapped infected fluid (pus), with resulting tubal distention. The findings are usually apparent at US, with characteristic thickening and hyperemia of the tubal wall and the presence of debris, with or without a fluid-debris level, within the dilated tube. At CT, pyosalpinx manifests either as a serpentine or tubular structure with a thick enhancing wall and complex internal fluid or as a complex cystic mass. Adjacent pelvic edema, periuterine and adnexal fat stranding, and the presence of free fluid in the cul-de-sac may also accompany the findings (Fig 8) (5). Clear identification of ovarian involvement with the infectious process may be difficult at CT, particularly if the degree of tubal distention is severe. MR imaging is a more sensitive modality for the detection of ovarian involvement. MR imaging also aids in the differentiation of pyosalpinx from hematosalpinx, because the latter will not demonstrate wall thickening and will show high or variable signal intensity on T1-weighted MR images because of the presence of blood products (24). As the inflammation subsides, the pus undergoes proteolysis, and the tube becomes filled with thin serous fluid, transforming from pyosalpinx into hydrosalpinx (20,25).

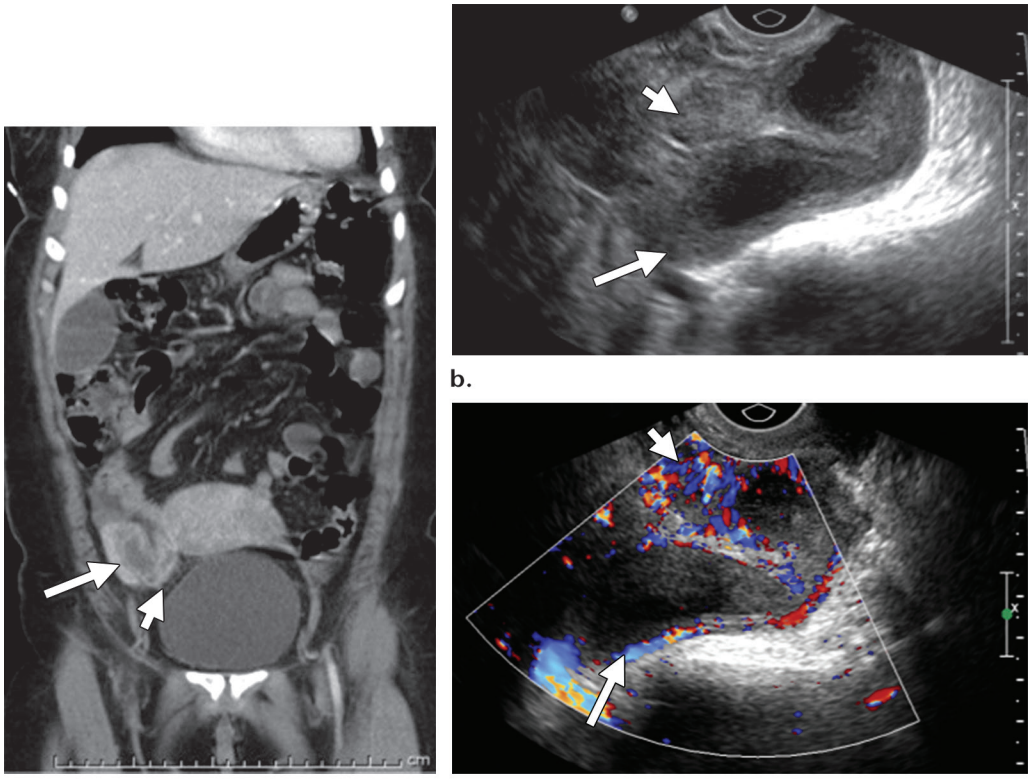

Figure 8. Pyosalpinx in a 48-year-old woman presenting with fever, right lower quadrant abdominal pain, and leukocytosis. **(a)** Coronal contrast-enhanced CT image shows a dilated right fallopian tube with a thick enhancing wall (long arrow) and peritubal fat stranding (short arrow), findings compatible with pyosalpinx. No frank tubo-ovarian abscess was depicted. **(b, c)** Corresponding transvaginal gray-scale **(b)** and color **(c)** US images show a dilated thick-walled right fallopian tube (long arrow) containing hyperechoic material, with surrounding hyperemia, findings compatible with pyosalpinx. Note the closely adherent hyperemic but small ovary (short arrow), which demonstrates an otherwise unremarkable parenchyma.

Hydrosalpinx

Hydrosalpinx occurs when a fallopian tube fills with serous fluid as a result of distal blockage. The most common cause of hydrosalpinx is previous episodes of PID. Other causes include endometriosis, peritubal adhesions from prior surgeries, tubal cancer, and prior tubal pregnancy (20,26). Symptoms of hydrosalpinx are variable, ranging from no symptoms to recurrent lower abdominal or pelvic pain. US is the first-line imaging modality for the diagnosis of hydrosalpinx, with characteristic findings of a dilated fallopian tube containing simple-appearing fluid. When distended, the tube folds on itself, which results in the formation of incomplete septa. A pathognomonic finding of hydrosalpinx at US, CT, and MR imaging is a "cogwheel" appearance of the tube when imaged in cross section, an appearance that is due to thickened longitudinal folds (23,27). Otherwise, the wall of the tube is thin and shows no appreciable enhancement or hyperemia (Fig 9) (28).

If the diameter of the tube reaches 10 cm, hydrosalpinx may mimic a multilocular ovarian tumor such as a cystadenoma. MR imaging may help to delineate adnexal structures and demonstrate the tubular nature of the mass with its characteristic folds that are separate from the normal-appearing ipsilateral ovary.

Tubo-ovarian Abscess

Tubo-ovarian abscess is one of the major and serious late complications of acute salpingitis and occurs in as many as 15% of women with PID. Tubo-ovarian abscess represents further progression of infection and inflammation, which results in the formation of a complex cystic and solid mass with complete destruction of the normal adnexal architecture. The ovary and fallopian tube can no longer be delineated. As many as 33% of women diagnosed with tubo-ovarian abscess require hospitalization (29). Tubo-ovarian abscesses are unilateral in 25%–50% of cases (30). Clinical symptoms of tubo-ovarian abscess at presentation are not substantially different from those of patients who are diagnosed with PID alone. Typically, patients with an abscess present with acute or chronic pelvic pain, fever, leukocytosis, and an adnexal mass. Patients may also report nausea, vomiting, a change in bowel

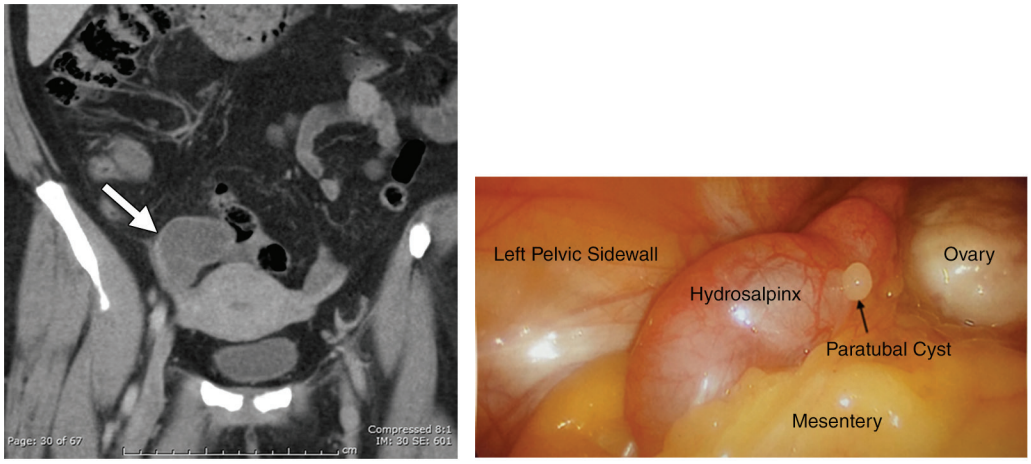

a. b.

Figure 9. Late PID: hydrosalpinx in two different patients. **(a)** Coronal contrast-enhanced CT image of a 50-year-old woman presenting with right lower quadrant pain shows a dilated fluid-filled right fallopian tube with a thin nonenhancing wall (arrow) and incomplete septa. **(b)** Intraoperative photograph of a 32-year-old woman shows a dilated fallopian tube and its relationship to the adjacent ovary, uterus, pelvic sidewall, and mesentery. Note the incidental finding of a small paratubal cyst.

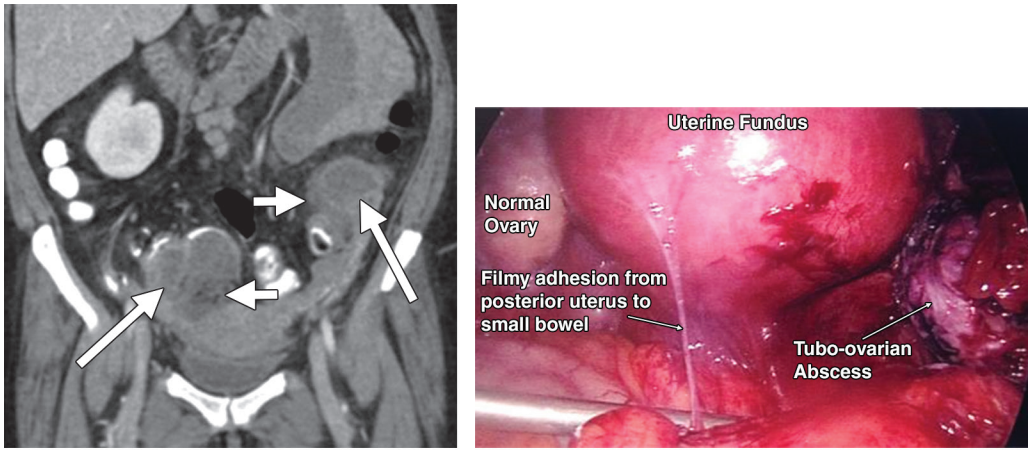

a. b.

Figure 10. Late PID: tubo-ovarian abscess in two different patients. **(a)** Coronal contrast-enhanced CT image of a 35-year-old woman presenting with pelvic pain and fever shows bilateral adnexal multilocular septate cystic masses (long arrows) with thick enhancing septa, loss of the normal ovarian parenchyma, and surrounding fat stranding (short arrows). **(b)** Intraoperative photograph of the posterior pelvis of a different woman shows a right complex hemorrhagic mass compatible with a tubo-ovarian abscess, with a prominent adhesion extending from the uterus to the small bowel. Note the normal-appearing left ovary.

habits, and vaginal discharge. In some cases, however, fever and leukocytosis may be absent.

Imaging is important for prompt diagnosis and treatment of tubo-ovarian abscess. On contrast material–enhanced CT images, the most common finding of a tubo-ovarian abscess is a multilocular septate cystic mass in the adnexa with a thick uniformly enhancing wall (Fig 10). Other common findings include a loss of fat planes between the mass and the adjacent pelvic organs, as well as thickening of the uterosacral ligaments and fluid in the cul-de-sac (31). On rare occasions, gas bubbles can be seen within the mass (5,12). US and MR imaging can further delineate the findings of tubo-ovarian abscess, demonstrating the complex nature of this process with destruction of the ovarian parenchyma. At MR imaging, abscesses usually have low signal intensity on T1-weighted MR images and high signal intensity on T2-weighted MR images, although imaging findings depend on the presence of hemorrhage and the protein content of the mass. A hyperintense rim along the inner wall of the abscess cavity can be seen on T1-weighted MR images, a finding attributed to formation of granulation tissue and hemorrhage (32).

When tubo-ovarian abscess is associated with ascites and lymphadenopathy, the abscess may be difficult to differentiate from ovarian malignancy

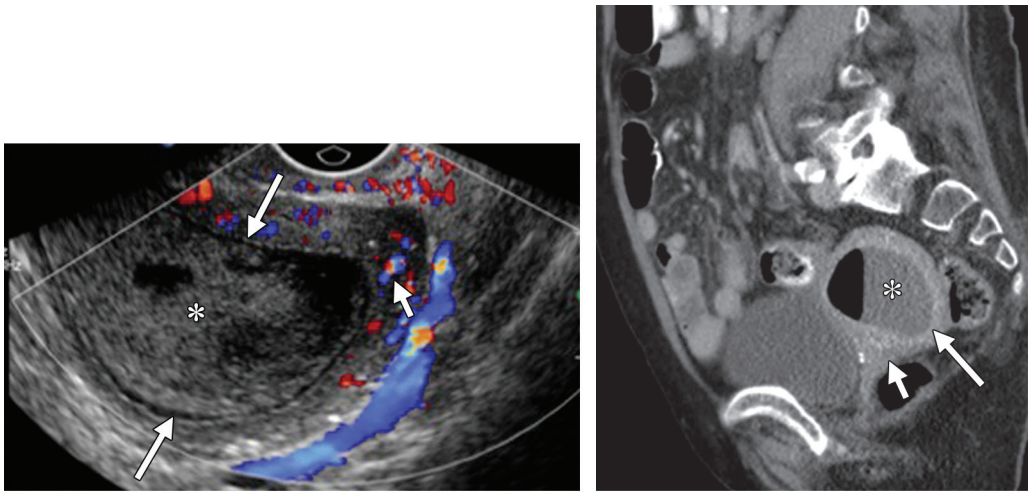

a. b.

Figure 11. Late PID: pyometra in a 52-year-old woman presenting with cervical motion tenderness and a thick yellow vaginal discharge. **(a)** Sagittal transvaginal color Doppler US image shows complex heterogeneous fluid (*) within a markedly dilated endometrial canal (long arrows) and hyperemia of the adjacent myometrium (short arrow). Uterine wall thinning is apparent. **(b)** Sagittal contrast-enhanced CT image from the same date shows a distended uterus (long arrow) containing complex fluid and an air-fluid level within the endometrial canal (*), hyperemic endometrium, and fat stranding and pelvic edema in the vesicouterine pouch (short arrow), findings compatible with endometritis and pyometra.

(33). Pelvic abscesses from other nongynecologic sources are other potential diagnostic considerations. Anterior displacement of the broad ligament, because of the posterior position of the mesovarium, may allow differentiation of a tubo-ovarian abscess from a pelvic abscess of other origin (12). In addition, pelvic abscesses originating from the appendix, colon, and bladder tend to have thicker walls and may be located further from the adnexa. At CT, tubo-ovarian abscess may be indistinguishable from pelvic endometriosis.

Pyometra

Pyometra represents a chronic form of endometritis that is characterized by accumulation of pus in the uterine cavity. In order for pyometra to develop, both an endometrial infection and blockage or stenosis of the cervix must be present, findings that result in impedance of the natural drainage of the uterine cavity. Pyometra has an incidence of 0.01%–0.5% among gynecologic patients and occurs primarily in the postmenopausal age group, with an incidence as high as 13.6% in this group (34). As many as 50% of patients are asymptomatic. If there are symptoms, patients may present with lower abdominal or suprapubic pain, rigors, fever, and the discharge of pus. CT findings include distention of the uterine cavity with complex fluid, inflammatory changes in the surrounding parametrial fat, and free fluid in the posterior cul-de-sac. Gas bubbles or an air-fluid level may be seen within the endometrial canal (Fig 11). Pyometra is treated with antibiotic therapy or surgery.

Complications of PID

Tubal Damage

A common and devastating long-term sequela of PID is damage to the fallopian tubes, manifested as scarring and adhesions within the tubal lumen and adhesions in the peritubal fat. Both of these factors are thought to play a major role in the development of ectopic pregnancies, with PID suspected to be involved in 30%–40% of cases (Fig 12). Because tubal function is impeded, resulting in tubal obstruction and development of hydrosalpinx, infertility is a common complication of PID, with 40%–50% of cases of infertility being attributable to this cause (5,6).

Tubo-ovarian Abscess Rupture and Peritonitis

Tubo-ovarian abscess can be complicated by rupture, which may result in life-threatening peritonitis (35) and acute respiratory distress syndrome. Despite modern medical and surgical management, mortality from a ruptured tubo-ovarian abscess remains as high as 5%–10% (36). CT findings of peritonitis include enhancement of the peritoneal folds, as well as thickening and enhancement of the fascial planes. Multiple abscesses may be seen throughout the peritoneal cavity (Fig 13). Ileus of the bowel is associated with tubo-ovarian abscess–induced peritonitis and should be differentiated from other causes. Tubo-ovarian abscess may also rarely form a fistula to the adjacent bowel or bladder, a finding that may be suspected when gas is detected within the tubo-

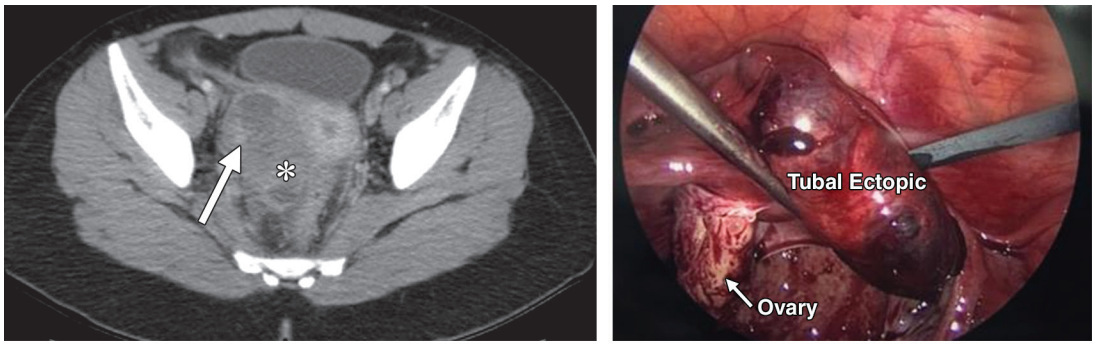

a. b.

Figure 12. Ectopic pregnancy in a 19-year-old woman with right lower quadrant pain. **(a)** Axial contrast-enhanced CT image shows a complex right adnexal mass (arrow), with anterior displacement of the broad ligament and surrounding lateral pelvic fat stranding (*). US disclosed a tubal ectopic pregnancy. **(b)** Intraoperative photograph shows a right tubal ectopic pregnancy.

a. b.

Figure 13. Perforated tubo-ovarian abscess in a 43-year-old woman with diabetes, abdominal pain, and fever. Axial **(a)** and coronal **(b)** contrast-enhanced CT images show bilateral tubo-ovarian abscesses (long white arrows) complicated by perforation of the left tubo-ovarian abscess with development of peritoneal fold enhancement (short white arrows on **b**), findings compatible with peritonitis, as well as a large complex fluid collection (*) with gas bubbles and an enhancing wall (black arrow on **b**) extending along the left iliopsoas muscle, findings compatible with an abscess.

ovarian abscess cavity and when there is focal wall thickening in the adjacent bowel.

Peritoneal Adhesions

Reactive inflammation associated with tubo-ovarian abscess and peritonitis can be responsible for the formation of peritoneal adhesions, a late complication of PID. Adhesions can lead to the development of ileus of the small or large bowel, bowel obstruction, or hydroureteronephrosis. The presence of an adnexal mass and/or pelvic fat stranding may point to the possible cause of bowel or ureteral obstruction.

Fitz-Hugh–Curtis Syndrome

Fitz-Hugh–Curtis syndrome, also known as perihepatitis, is a rare complication of PID that is seen in 1%–30% of cases (37,38). This condition is defined as inflammation of the peritoneal capsule of the liver and is believed to result from peritoneal spread of pelvic infection along the right paracolic gutter. Women may present with rapid onset of sharp right upper quadrant pain and tenderness. The differential diagnosis at presentation commonly includes acute cholecystitis and pleurisy (39). At contrast-enhanced CT, Fitz-Hugh–Curtis syndrome is characterized by intense enhancement and thickening of the anterior liver capsule. Inflammation of the capsule may also cause geographic areas of variable perfusion in the subcapsular and periportal locations. Fluid and fat stranding can be seen extending from the pelvis into the right upper quadrant by way of the paracolic gutter.

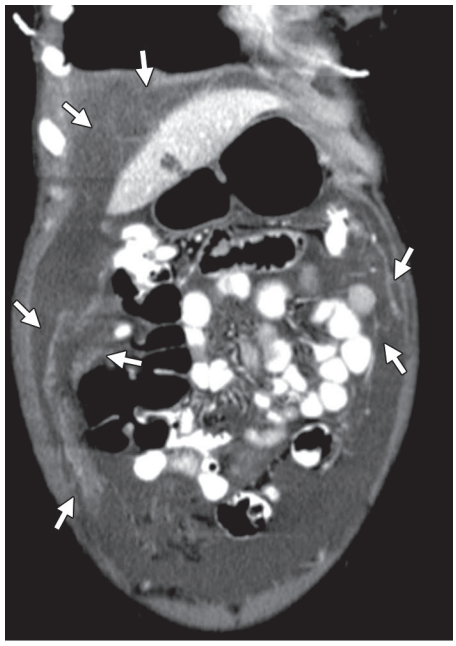

a.

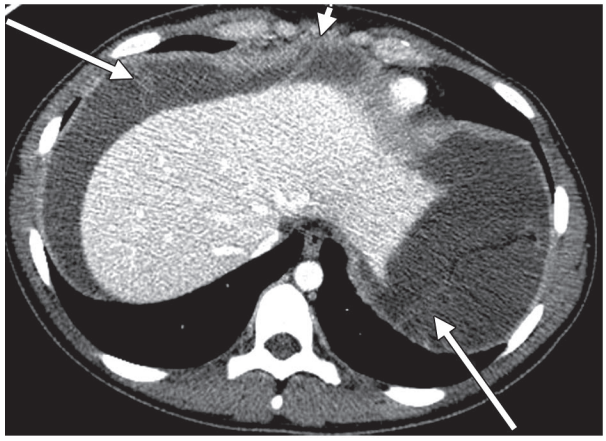

b.

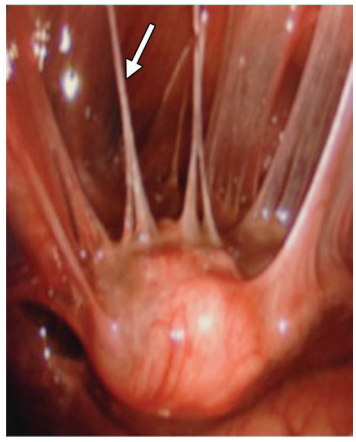

c.

Figure 14. Fitz-Hugh–Curtis syndrome in a 35-year-old woman. **(a, b)** Coronal **(a)** and axial **(b)** CT images show peritoneal septa (arrows) along the paracolic gutters and loculated perihepatic fluid, findings compatible with multiple adhesions. A large amount of ascites is also depicted. **(c)** Intraoperative photograph shows classic "violin-string" adhesions (arrow) along the hepatic capsule.

Peritoneal septa and loculated perihepatic fluid may be seen, and gallbladder wall thickening may also be depicted (Fig 14a, 14b) (40,41). Multiple classic "violin string" adhesions may be found between the liver capsule and the anterior abdominal wall during intraoperative exploration (Fig 14c). Isolation of *N gonorrhoeae* and *C trachomatis* in a cervical smear or in peritoneal fluid supports the diagnosis (42). No known long-term complications of this disorder have been observed (37).

Ovarian Vein Thrombophlebitis

Ovarian vein thrombophlebitis may occur as a complication of PID. The right ovarian vein is the affected vessel in 80%–90% of cases. Contrast-enhanced CT demonstrates a distended ovarian vein with an enhancing wall and with low-attenuation intraluminal filling defects (Fig 15) (43). Lack of enhancement of the vein will be observed if the entire vessel is occluded. Associated inflammatory changes may be seen in the pelvic fat, often accompanied by free fluid. If unrecognized or left untreated, ovarian vein thrombophlebitis may result in septic pulmonary emboli (44).

Uterine Rupture

Uterine rupture is a devastating complication of pyometra, a complication that is due to the accumulation of pus within the endometrial canal and impaired drainage by way of the cervical canal. The accumulation of secretions may lead to gradual uterine enlargement and focal thinning of the uterine wall, which may then become necrotic, slough, and result in focal perforation (Fig 16) (45). Perforation most commonly occurs in the uterine fundus and results in development of diffuse peritonitis, which can be difficult to distinguish from other causes of a perforated viscus (46). Multiplanar reformatted images are partic-

Figure 15. Left ovarian thrombosis in a 36-year-old woman with pelvic pain and leukocytosis. Coronal contrast-enhanced CT image shows a filling defect in the left ovarian vein, with associated vessel wall enhancement (arrow). Hyperemia in the left ovary and fallopian tube was better seen at subsequent US.

Figure 16. Ruptured pyometra in an 82-year-old woman with abdominal pain and a history of actinomycosis, who now presented with a purulent vaginal discharge. Axial contrast-enhanced CT image shows an abnormally dilated and fluid-filled endometrial cavity (white arrow) with an adjacent peripherally enhancing abscess (black arrow) containing an air-fluid level. Note the thinning of the uterine wall adjacent to the abscess, as well as the presacral fat stranding (*).

ularly helpful in localizing the site of perforation and assessing periuterine abscesses. Peritonitis secondary to uterine rupture of pyometra should be considered as a surgical emergency, and immediate laparotomy must be performed to avoid the complications of generalized peritonitis, such as septic shock (47).

Mimics of PID

Careful CT assessment of common PID mimics will help avoid misinterpretation, delay in management, and unnecessary surgery. Pathologic processes that have findings similar to those of PID include endometriosis, adnexal torsion, ruptured hemorrhagic ovarian cyst, adnexal neoplasms, appendicitis, and diverticulitis (Table).

Pelvic Endometriosis or Endometrioma

Endometriosis is a common cause of pelvic pain and infertility, with as many as 30% of women with endometriosis demonstrating tubal involvement at laparoscopy (20,48). Ruptured deep pelvic endometriomas release blood products that cause adhesions and fibrosis, which may lead to findings that can mimic PID, such as the development of complex pelvic masses, nodularity of the uterosacral ligaments, and peritubal adhesions with tubal obstruction (49,50). The CT appearance of endometriomas can be nonspecific (51–53), although the presence of multiple complex lesions, high-attenuation components within the mass, and hematosalpinx help to narrow the differential diagnosis. Solid invasive endometriosis, which is commonly found in the rectouterine pouch or posterior cul-de-sac, often extends to or invades the posterior myometrium and can mimic an adhesion from previous PID (Fig 17) (54). At MR imaging, the presence of T1 hyperintensity within the lesions or in the fallopian tube can help confirm the diagnosis of endometriosis and differentiate it from PID (54).

Isolated Fallopian Tube Torsion

Isolated fallopian tube torsion is an extremely rare mimic of PID, affecting female adolescents and women of reproductive age. Presenting symptoms include acute onset of lower abdominal pain accompanied by nausea, vomiting, and peritoneal signs. At CT and US, the tube may appear twisted and/or dilated with tapered ends (the so-called beak sign), and the walls of the fallopian tube may be thickened and enhancing. The ipsilateral ovary is usually normal in size and structure and is found in its normal expected location. MR imaging can aid in the delineation of these anatomic structures and can help differentiate fallopian tube torsion from PID when US and CT findings are inconclusive (55).

Ovarian Torsion

Ovarian torsion is another common entity that can mimic PID at clinical examination and on images. Common CT imaging features that distinguish ovarian torsion from PID include an enlarged ovary with a diameter of more than 5 cm, a lack of ovarian contrast enhancement, and uterine deviation toward the affected side (56) (Fig 18). Fallopian tube thickening, obliteration of fat planes, and ascites can be present in both of these entities. When there is hemorrhagic infarction of the ovary, an adnexal hematoma may be detected. On rare occasions, gas may be seen within the twisted mass (57–59).

Pathologic Processes Mimicking PID

Mimic of PID	Clinical Manifestations	Mechanism of Action	Common Features with PID	Differentiating Features from PID
Pelvic endometriosis or endometrioma	Infertility, pelvic pain, dyspareunia	Recurrent hemorrhage within serosal implants leading to formation of peritubal adhesions and tubal obstruction	Complex hypoattenuating mass, nodularity and thickening of the uterosacral ligaments, peritubal and/or periuteral adhesions, dilated fallopian tubes	CT: multiple lesions, hyperattenuating component within the lesion, with or without hematosalpinx; US: complex cyst filled with uniform low-level internal echoes, with or without flow on color Doppler images, bowel tethering; MR imaging: T1 hyperintensity within the implants, T1 hyperintensity within the dilated tube consistent with hematosalpinx
Isolated fallopian tube torsion	Acute onset of lower abdominal pain radiating to the groin, associated with nausea, vomiting, and peritoneal signs	Lymphatic and venous congestion leading to fallopian tube fimbrial end engorgement, which serves as a lead point for torsion	Free fluid, dilated fallopian tube, peritubal stranding, thickening of the broad ligament	CT, US, MR imaging: fusiform dilatation of fallopian tube with tapered ends ("beak sign"); fallopian tube may appear twisted, with or without thickening and enhancement of the fallopian tube wall, with or without hyperattenuating or T1-hyperintense material within the fallopian tube lumen caused by hemorrhage; normal ipsilateral ovary
Ovarian torsion	Severe pelvic pain, which may be intermittent with torsion and detorsion; vomiting and fever if ovary is infarcted	Partial or complete rotation of the ovarian vascular pedicle, resulting in obstruction of ovarian venous outflow and/or arterial inflow; 50%–90% associated with a mass that serves as a lead point	Fallopian tube thickening, obliteration of fat planes, with or without ascites, with or without complex adnexal mass, with or without enlarged ovaries (oophoritis)	CT, MR imaging: enlarged ovary (>5 cm) with decreased or absent enhancement, in an abnormal location, twisted pedicle, uterine deviation toward the affected side, with or without hemoperitoneum; US: enlarged ovary, hyperechoic stroma with peripherally displaced follicles, twisted pedicle ("whirlpool sign"), absent venous flow
Hemorrhagic ovarian cyst	Asymptomatic or acute abdominal pain	Commonly results from bleeding into a corpus luteum or follicular cyst	Complex adnexal cyst, with or without free fluid	CT, MR imaging: ring of peripheral enhancement and internal hyperattenuating or hyperintense component, with or without fluid-fluid level, with or without hemoperitoneum, absent fallopian tube thickening or distention; US: avascular hypoechoic crenulated cyst with lacy interstices, retracted clot may show jellylike motion with transducer compression, peripheral "ring of fire" on color Doppler images
Ovarian neoplasm	Pelvic mass, pelvic pain, increased abdominal girth, associated with elevated CA-125 level (80% have CA-125 levels > 35 U/mL)	Benign and malignant cystic or cystic and solid ovarian neoplasms, family history, multifactorial, malignant ascites likely resulting from combination of impaired lymphatic drainage and increased vascular permeability	Multiple cystic masses, often bilateral, with or without ascites	CT, MR imaging: enhancing solid/papillary components, thick wall, and septa, with or without peritoneal carcinomatosis and lymphadenopathy, fallopian tube usually intact; US: complex cystic masses with thick walls, septa, and papillary projections that show flow on color Doppler images
Fallopian tube neoplasm	Colicky lower abdominal pain (caused by partial tube obstruction); intermittent profuse serosanguineous vaginal discharge; pain is relieved by discharge; vaginal bleeding and spotting	Rare neoplasms; etiology unknown; hormonal, reproductive, and genetic factors may be risk factors	Dilated tube, with or without fat stranding, with or without ascites; ovary is intact	CT, MR imaging: if associated with hydrosalpinx, mixed solid and cystic adnexal mass or tubular cystic structure with papillary projections; attenuation or signal intensity tends to be equal to that of other soft tissues, and enhancement is less than that of myometrium; US: sausage-shaped solid mass or cystic tubular structure with mural nodules, solid components show blood flow on color Doppler images
Appendicitis	Periumbilical pain migrating to right lower quadrant, anorexia, vomiting, nausea, with or without leukocytosis	Inflammation of the appendix caused by luminal obstruction and superimposed infection (obstruction commonly caused by appendicolith)	Cystic right adnexal tubular structure, fat stranding, with or without ascites, hyperemic wall, with or without complex fluid collection (if perforated)	CT, MR imaging: dilated and blind-ending tubular structure arising from the cecum, thickening of the cecal wall ("cecal bar" sign); US: distended (>7 mm), thick-walled, and noncompressible shadowing hyperechoic appendicolith
Perforated diverticulitis with abscess formation	Nausea, vomiting, fever, leukocytosis, rebound tenderness, diffuse lower abdominal pain	Intramural and pericolonic infectious or inflammatory process resulting from perforation of colonic diverticula	Complex cystic collections, fat stranding	CT, MR imaging: bowel thickening associated with inflamed diverticula, with or without extraluminal air, with or without fistula to the adjacent organs

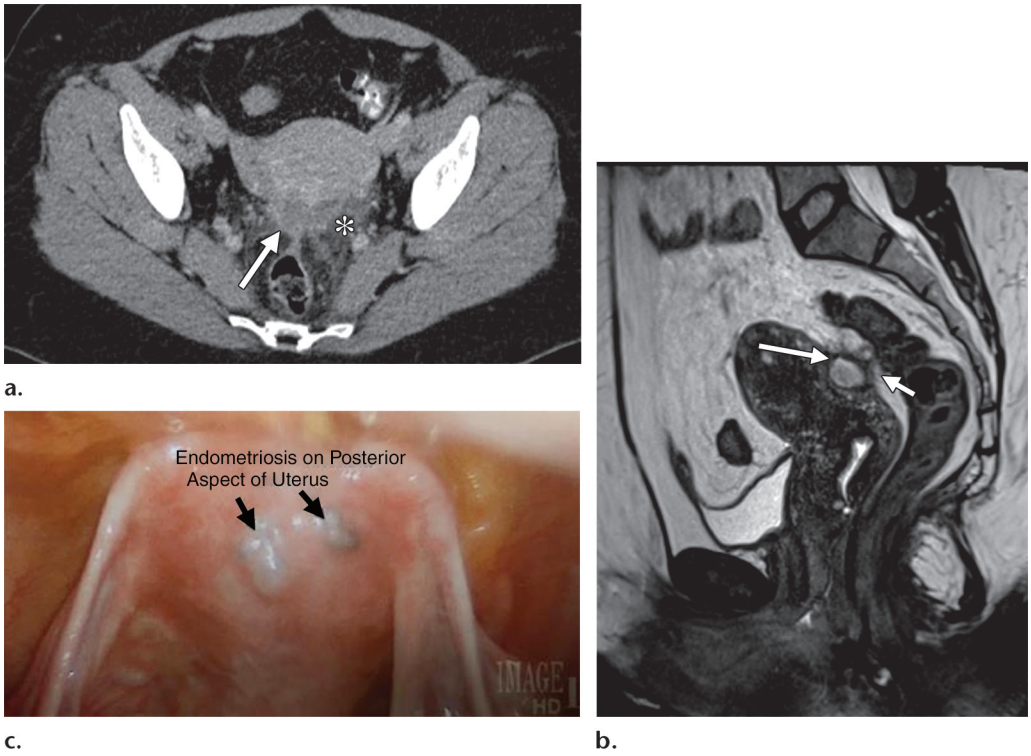

Figure 17. Endometriosis in a 32-year-old woman with pelvic pain and dyspareunia. **(a)** Axial contrast-enhanced CT image shows abnormal increased attenuation in the cul-de-sac (arrow), with surrounding inflammatory stranding (*). **(b)** Sagittal T2-weighted MR image shows a T2-hyperintense focus (long arrow) coating the posterior uterine surface, with tethering of the adjacent sigmoid colon (short arrow), findings consistent with endometriosis. **(c)** Intraoperative photograph shows the presence of endometrial implants (arrows).

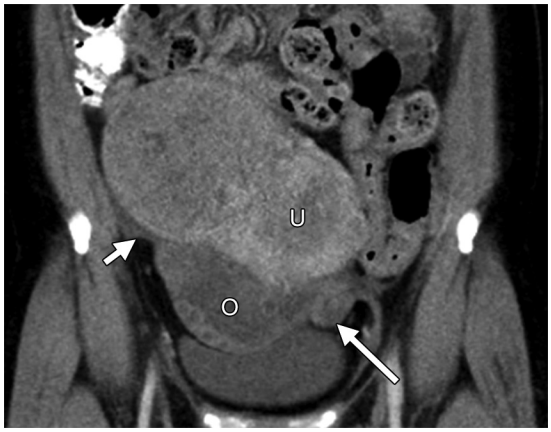

Figure 18. Ovarian torsion mimicking oophoritis in a 36-year-old woman presenting with left acute pelvic pain. Coronal contrast-enhanced CT image shows an enlarged left ovary *(O)* that could mimic oophoritis; however, its abnormal location on the right, the lack of enhancement, the displacement of peripheral follicles, and the twisting of its vascular pedicle (long arrow) are consistent with ovarian torsion. Note the enlarged fibroid uterus *(U)* and the trace free fluid (short arrow). At surgery, a 720° twist of the vascular pedicle with a nonviable left ovary was found.

Hemorrhagic Ovarian Cyst

Complex cystic adnexal lesions, including hemorrhagic cysts, are common mimics of PID. Clinical manifestations are frequently nonspecific and unhelpful in distinguishing between these entities. Characteristic features of hemorrhagic cysts include the presence of a unilocular or, less commonly, a bilocular adnexal cyst with a ring of peripheral contrast enhancement and an internal high-attenuation component with or without a fluid-hematocrit level. Hemoperitoneum is present if the cyst ruptures (60,61). Differentiation of hemorrhagic cysts from PID can be made on the basis of hemoperitoneum and the absence of tubular thickening or tubular distention. Vaginal specimens are helpful in the exclusion of infectious processes.

Ovarian Neoplasms

The differentiation of serous cystadenomas and malignant ovarian neoplasms from a complicated tubo-ovarian abscess can pose a diagnostic challenge. The key imaging findings suggestive of malignancy include a lobulated solid or complex mass larger than 4 cm in diameter, enhancing papillary projections, and walls and/or septa that measure more than 3 mm thick (Fig 19) (62). Multiplanar reformatted images may facilitate recognition of the tubular nature of a complex mass, thus helping to identify it as a tubo-ovarian abscess.

Figure 19. Ovarian neoplasm in a 63-year-old woman with pelvic pain and early satiety. Axial contrast-enhanced CT image shows enlarged heterogeneous ovaries (arrows) and free fluid (*). No fat stranding or dilated tubes are depicted. The findings at histopathologic examination disclosed bilateral serous cystadenofibromas.

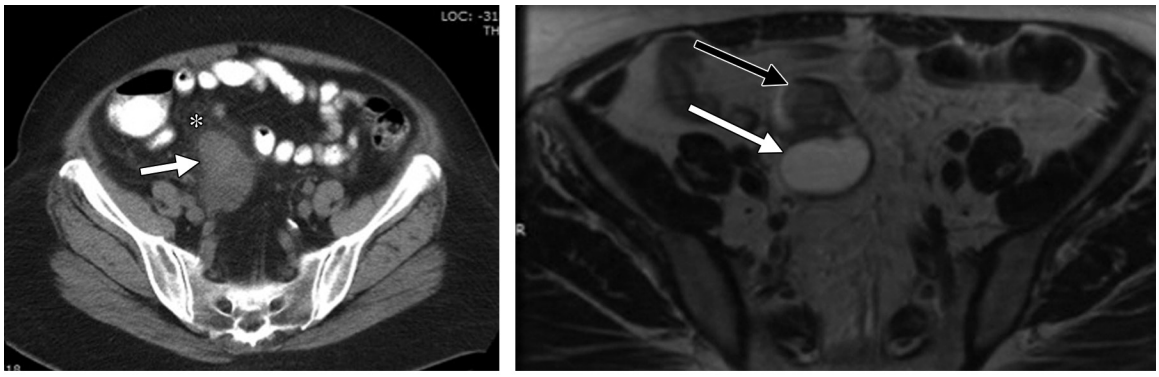

a. **b.**

Figure 20. Fallopian tube carcinoma in a 46-year-old woman with lower abdominal pain, no fever, and a history of right oophorectomy. **(a)** Axial nonenhanced CT image shows a right adnexal mass (arrow) with surrounding anterior pelvic fat stranding (*). **(b)** Axial T2-weighted MR image shows the right solid and cystic adnexal mass consisting of a dilated fallopian tube (white arrow) with an adjacent solid component (black arrow), findings raising the suspicion of a neoplasm obstructing the tube. The solid component demonstrated enhancement on gadolinium-enhanced images (not shown). The findings at histopathologic examination disclosed fallopian tube carcinoma.

Fallopian Tube Neoplasms

Primary fallopian tube neoplasms are extremely rare, affecting postmenopausal women and accounting for no more than 1% of all gynecologic malignancies (63). Patients may present with vaginal bleeding and/or pelvic pain. Most fallopian tube neoplasms are solid and may have small cystic components that are due to necrosis and hemorrhage. When the neoplasm is associated with hydrosalpinx, the entire lesion appears as a large mass with mixed cystic and solid components (64). US, CT, and MR imaging findings are nonspecific and may be mistaken for tubo-ovarian abscess, ovarian neoplasm, or uterine leiomyoma. Contrast enhancement of the solid components helps to differentiate the neoplastic portion from hydrosalpinx (Fig 20).

Appendicitis

The differentiation of PID from appendicitis may be challenging on a clinical basis. The identification of mural nodules, corresponding to thickened endosalpingian folds, may help to identify the fallopian tube at CT and US (44). The presence of an appendicolith, cecal origin of the tubular structure, and the presence of cecal wall thickening ("cecal bar" sign) are helpful distinguishing features of appendicitis (Fig 21). Investigators have reported that the presence of periovarian fat stranding, a thickened rectosigmoid wall, and a normal-appearing cecum in young female patients favors the diagnosis of tubo-ovarian abscess, as opposed to appendicitis (65). In addition, in cases of tubo-ovarian abscess, the round ligament may be anteriorly displaced, and satellite lesions are often seen adjacent to the primary tubo-ovarian abscess (66).

Diverticulitis

Acute diverticulitis typically occurs in older patients but can occasionally be seen in premenopausal female patients. PID and diverticulitis may be indistinguishable on clinical grounds. Differentiation on the basis of imaging findings may also be difficult if inflammatory changes from acute diverticulitis extend to involve the ipsilateral adnexa or if diverticulitis is complicated by abscess formation. In general, abscesses related to a perforated

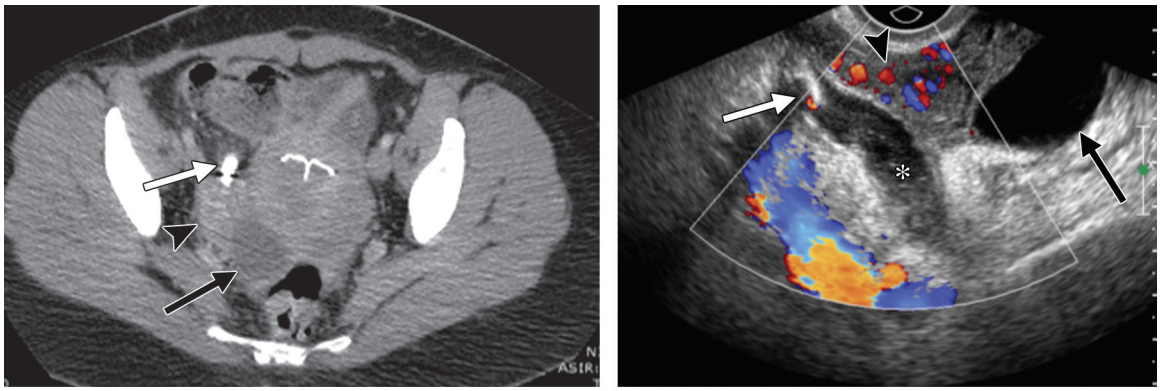

a. b.

Figure 21. Appendicitis in a 37-year-old woman with right lower quadrant pain, nausea, vomiting, and chills for 2 days. **(a)** Axial contrast-enhanced CT image shows an appendicolith (white arrow) within a poorly defined right adnexal tubular fluid-filled structure compatible with an inflamed appendix (not shown). Note the adjacent reactive thickening of the right fallopian tube (arrowhead) and the loculated fluid (black arrow) in the right adnexa. **(b)** Transvaginal color Doppler US image (obtained the same day as image in **a**) again shows an appendicolith (white arrow) within the dilated appendix (*), a hyperemic and thickened right fallopian tube (arrowhead), and a right ovarian cyst (black arrow) corresponding to the loculated fluid at CT.

bowel tend to have thicker walls. Extraluminal air, inflamed diverticula, and fistula formation favor the diagnosis of diverticulitis rather than PID (67).

Conclusion

PID is an important and prevalent pelvic infection among women of reproductive age. CT is often the first imaging modality used for evaluation of patients with PID, because the presenting symptoms are vague and nonspecific. An awareness of the various CT imaging findings of early and late PID and their associated complications is crucial to prevent misdiagnosis and ensure optimal patient care. Early detection of PID can reduce the subsequent risk of tube-related infertility, ectopic pregnancy, and pelvic adhesions resulting in chronic pelvic pain. Recognition and prompt treatment of this disease can decrease the rate of complications such as tubo-ovarian abscess, uterine perforation, bowel obstruction, and hydroureteronephrosis.

Acknowledgments.—The authors thank Mark Saba, Campus Community Technologies–Yale ITS, New Haven, Conn, for his assistance with the illustrations; Henry R. Douglas, Photography and Digital Services, Yale University School of Medicine, New Haven, Conn, for his help with the images; and Denise P. Hersey, Cushing/Whitney Medical Library, Yale University School of Medicine, New Haven, Conn, for assistance with the literature.

References

1. Curtis KM, Hillis SD, Kieke BA Jr, Brett KM, Marchbanks PA, Peterson HB. Visits to emergency departments for gynecologic disorders in the United States, 1992-1994. Obstet Gynecol 1998;91(6):1007–1012.
2. Goyal M, Hersh A, Luan X, Localio R, Trent M, Zaoutis T. National trends in pelvic inflammatory disease among adolescents in the emergency department. J Adolesc Health 2013;53(2):249–252.
3. Centers for Disease Control and Prevention. Pelvic inflammatory disease (PID): CDC fact sheet—detailed version. CDC Web site. http://www.cdc.gov/std/pid/stdfact-pid-detailed.htm. Published 2014. Accessed February 3, 2015.
4. Soper DE. Pelvic inflammatory disease. Obstet Gynecol 2010;116(2 pt 1):419–428.
5. Sam JW, Jacobs JE, Birnbaum BA. Spectrum of CT findings in acute pyogenic pelvic inflammatory disease. RadioGraphics 2002;22(6):1327–1334.
6. McCormack WM. Pelvic inflammatory disease. N Engl J Med 1994;330(2):115–119.
7. Moore KL, Agur AMR, Dalley AF. Essential clinical anatomy. 4th ed. Baltimore, Md: Lippincott Williams & Wilkins, 2011.
8. Levenson RB, Camacho MA, Horn E, Saghir A, McGillicuddy D, Sanchez LD. Eliminating routine oral contrast use for CT in the emergency department: impact on patient throughput and diagnosis. Emerg Radiol 2012;19(6):513–517.
9. Wilbur A. Computed tomography of tuboovarian abscesses. J Comput Assist Tomogr 1990;14(4):625–628.
10. Lee MH, Moon MH, Sung CK, Woo H, Oh S. CT findings of acute pelvic inflammatory disease. Abdom Imaging 2014;39(6):1350–1355.
11. Jung SI, Kim YJ, Park HS, Jeon HJ, Jeong KA. Acute pelvic inflammatory disease: diagnostic performance of CT. J Obstet Gynaecol Res 2011;37(3):228–235.
12. Wilbur AC, Aizenstein RI, Napp TE. CT findings in tuboovarian abscess. AJR Am J Roentgenol 1992;158(3):575–579.
13. Langer JE, Dinsmore BJ. Computed tomographic evaluation of benign and inflammatory disorders of the female pelvis. Radiol Clin North Am 1992;30(4):831–842.
14. Bin Park S, Lee JH, Lee YH, Song MJ, Choi HJ. Multilocular cystic lesions in the uterine cervix: broad spectrum of imaging features and pathologic correlation. AJR Am J Roentgenol 2010;195(2):517–523.
15. Okamoto Y, Tanaka YO, Nishida M, Tsunoda H, Yoshikawa H. Pelvic imaging: multicystic uterine cervical lesions—can magnetic resonance imaging differentiate benignancy from malignancy? Acta Radiol 2004;45(1):102–108.
16. Apter S, Shmamann S, Ben-Baruch G, Rubinstein ZJ, Barkai G, Hertz M. CT of pelvic infection after cesarean section. Clin Exp Obstet Gynecol 1992;19(3):156–160.
17. Van Hoe L, Gryspeerdt S, Amant F, Marchal G, Baert AL, Spitz B. Abdominal pain in the postpartum: role of imaging. J Belge Radiol 1995;78(3):186–189.
18. Twickler DM, Setiawan AT, Harrell RS, Brown CE. CT appearance of the pelvis after cesarean section. AJR Am J Roentgenol 1991;156(3):523–526.
19. Haggerty CL, Hillier SL, Bass DC, Ness RB; PID Evaluation and Clinical Health Study investigators. Bacterial vaginosis and anaerobic bacteria are associated with endometritis. Clin Infect Dis 2004;39(7):990–995.
20. Kim MY, Rha SE, Oh SN, et al. MR imaging findings of hydrosalpinx: a comprehensive review. RadioGraphics 2009;29(2):495–507.
21. Potter AW, Chandrasekhar CA. US and CT evaluation of acute pelvic pain of gynecologic origin in nonpregnant premenopausal patients. RadioGraphics 2008;28(6):1645–1659.

22. Taipale P, Tarjanne H, Ylostalo P. Transvaginal sonography in suspected pelvic inflammatory disease. Ultrasound Obstet Gynecol 1995;6(6):430–434.
23. Tukeva TA, Aronen HJ, Karjalainen PT, Molander P, Paavonen T, Paavonen J. MR imaging in pelvic inflammatory disease: comparison with laparoscopy and US. Radiology 1999;210(1): 209–216.
24. Rezvani M, Shaaban AM. Fallopian tube disease in the nonpregnant patient. RadioGraphics 2011;31(2):527–548.
25. Blaustein A, ed. Pathology of the female genital tract. 2nd ed. New York, NY: Springer-Verlag, 1982.
26. Outwater EK, Siegelman ES, Chiowanich P, Kilger AM, Dunton CJ, Talerman A. Dilated fallopian tubes: MR imaging characteristics. Radiology 1998;208(2):463–469.
27. Timor-Tritsch IE, Lerner JP, Monteagudo A, Murphy KE, Heller DS. Transvaginal sonographic markers of tubal inflammatory disease. Ultrasound Obstet Gynecol 1998;12(1):56–66.
28. Yamashita Y, Torashima M, Hatanaka Y, et al. Adnexal masses: accuracy of characterization with transvaginal US and precontrast and postcontrast MR imaging. Radiology 1995; 194(2):557–565.
29. Landers DV, Sweet RL. Tubo-ovarian abscess: contemporary approach to management. Rev Infect Dis 1983;5(5): 876–884.
30. Stenchever MA. Comprehensive gynecology. 4th ed. St Louis, Mo: Mosby, 2001.
31. Hiller N, Appelbaum L, Simanovsky N, Lev-Sagi A, Aharoni D, Sella T. CT features of adnexal torsion. AJR Am J Roentgenol 2007;189(1):124–129.
32. Imaoka I, Wada A, Matsuo M, Yoshida M, Kitagaki H, Sugimura K. MR imaging of disorders associated with female infertility: use in diagnosis, treatment, and management. RadioGraphics 2003;23(6):1401–1421.
33. Ha HK, Lim GY, Cha ES, et al. MR imaging of tubo-ovarian abscess. Acta Radiol 1995;36(5):510–514.
34. Sawabe M, Takubo K, Esaki Y, Hatano N, Noro T, Nokubi M. Spontaneous uterine perforation as a serious complication of pyometra in elderly females. Aust N Z J Obstet Gynaecol 1995;35(1):87–91.
35. Yitta S, Hecht EM, Slywotzky CM, Bennett GL. Added value of multiplanar reformation in the multidetector CT evaluation of the female pelvis: a pictorial review. RadioGraphics 2009;29(7): 1987–2003.
36. Rock JA, Jones HW III, eds. Te Linde's operative gynecology. 9th ed. Philadelphia, Pa: Lippincott Williams & Wilkins, 2003.
37. Lareau SM, Beigi RH. Pelvic inflammatory disease and tubo-ovarian abscess. Infect Dis Clin North Am 2008;22(4): 693–708, vii.
38. Sweet RL. Pelvic inflammatory disease. In: Sweet RL, Gibbs RS, eds. Infectious diseases of the female genital tract. 4th ed. Philadelphia, Pa: Lippincott Williams & Wilkins, 2002; 368–412.
39. Kim S, Kim TU, Lee JW, et al. The perihepatic space: comprehensive anatomy and CT features of pathologic conditions. RadioGraphics 2007;27(1):129–143.
40. Pickhardt PJ, Fleishman MJ, Fisher AJ. Fitz-Hugh–Curtis syndrome: multidetector CT findings of transient hepatic attenuation difference and gallbladder wall thickening. AJR Am J Roentgenol 2003;180(6):1605–1606.
41. Tsubuku M, Hayashi S, Terahara A, Furukawa T, Ohmura G. Fitz-Hugh-Curtis syndrome: linear contrast enhancement of the surface of the liver on CT. J Comput Assist Tomogr 2002;26(3):456–458.
42. Wølner-Hanssen P, Svensson L, Weström L, Mårdh PA. Isolation of *Chlamydia trachomatis* from the liver capsule in Fitz-Hugh-Curtis syndrome. N Engl J Med 1982;306(2): 113–114.
43. Urban BA, Pankov BL, Fishman EK. Postpartum complications in the abdomen and pelvis: CT evaluation. Crit Rev Diagn Imaging 1999;40(1):1–21.
44. Bennett GL, Harvey WB, Slywotzky CM, Birnbaum BA. CT of the acute abdomen: gynecologic etiologies. Abdom Imaging 2003;28(3):416–432.
45. Yildizhan B, Uyar E, Sişmanoğlu A, Güllüoğlu G, Kavak ZN. Spontaneous perforation of pyometra. Infect Dis Obstet Gynecol 2006;2006:26786. http://www.ncbi.nlm.nih.gov/pmc/articles/PMC1581463/. Published online March 29, 2006.
46. Stunell H, Hou D, Finlayson S, Harris AC. Spontaneous perforation of pyometra due to acute necrotising endometritis. J Obstet Gynaecol 2011;31(7):673–674.
47. Abu-Zaid A, Alomar O, Nazer A, Azzam A, Abudan Z, Al-Badawi I. Generalized peritonitis secondary to spontaneous perforation of pyometra in a 63-year-old patient. Case Rep Obstet Gynecol 2013;2013:929407. http://www.ncbi.nlm.nih.gov/pmc/articles/PMC3773424/. Published online August 29, 2013.
48. Gougoutas CA, Siegelman ES, Hunt J, Outwater EK. Pelvic endometriosis: various manifestations and MR imaging findings. AJR Am J Roentgenol 2000;175(2):353–358.
49. Friedman H, Vogelzang RL, Mendelson EB, Neiman HL, Cohen M. Endometriosis detection by US with laparoscopic correlation. Radiology 1985;157(1):217–220.
50. Bazot M, Gasner A, Ballester M, Daraï E. Value of thin-section oblique axial T2-weighted magnetic resonance images to assess uterosacral ligament endometriosis. Hum Reprod 2011;26(2):346–353.
51. Woodward PJ, Sohaey R, Mezzetti TP Jr. Endometriosis: radiologic-pathologic correlation. RadioGraphics 2001;21 (1):193–216.
52. Umaria N, Olliff JF. Imaging features of pelvic endometriosis. Br J Radiol 2001;74(882):556–562.
53. Buy JN, Ghossain MA, Mark AS, et al. Focal hyperdense areas in endometriomas: a characteristic finding on CT. AJR Am J Roentgenol 1992;159(4):769–771.
54. Siegelman ES, Oliver ER. MR imaging of endometriosis: ten imaging pearls. RadioGraphics 2012;32(6):1675–1691.
55. Gross M, Blumstein SL, Chow LC. Isolated fallopian tube torsion: a rare twist on a common theme. AJR Am J Roentgenol 2005;185(6):1590–1592.
56. Chang HC, Bhatt S, Dogra VS. Pearls and pitfalls in diagnosis of ovarian torsion. RadioGraphics 2008;28(5):1355–1368.
57. Bennett GL, Slywotzky CM, Giovanniello G. Gynecologic causes of acute pelvic pain: spectrum of CT findings. RadioGraphics 2002;22(4):785–801.
58. Rha SE, Byun JY, Jung SE, et al. CT and MR imaging features of adnexal torsion. RadioGraphics 2002;22(2):283–294.
59. Kawahara Y, Fukuda T, Futagawa S, et al. Intravascular gas within an ovarian tumor: a CT sign of ovarian torsion. J Comput Assist Tomogr 1996;20(1):154–156.
60. Wilbur AC, Goldstein LD, Prywitch BA. Hemorrhagic ovarian cysts in patients on anticoagulation therapy: CT findings. J Comput Assist Tomogr 1993;17(4):623–625.
61. Hallatt JG, Steele CH Jr, Snyder M. Ruptured corpus luteum with hemoperitoneum: a study of 173 surgical cases. Am J Obstet Gynecol 1984;149(1):5–9.
62. Kawamoto S, Urban BA, Fishman EK. CT of epithelial ovarian tumors. RadioGraphics 1999;19(Spec Issue): S85–S102.
63. Slanetz PJ, Whitman GJ, Halpern EF, Hall DA, McCarthy KA, Simeone JF. Imaging of fallopian tube tumors. AJR Am J Roentgenol 1997;169(5):1321–1324.
64. Kawakami S, Togashi K, Kimura I, et al. Primary malignant tumor of the fallopian tube: appearance at CT and MR imaging. Radiology 1993;186(2):503–508.
65. Eshed I, Halshtok O, Erlich Z, et al. Differentiation between right tubo-ovarian abscess and appendicitis using CT: a diagnostic challenge. Clin Radiol 2011;66(11):1030–1035.
66. Jeong WK, Kim Y, Song SY. Tubo-ovarian abscess: CT and pathological correlation. Clin Imaging 2007;31(6): 414–418.
67. Singh AK, Gervais DA, Hahn PF, Sagar P, Mueller PR, Novelline RA. Acute epiploic appendagitis and its mimics. RadioGraphics 2005;25(6):1521–1534.